ROMAI J., v.13, no.1(2017), 1–9

A WELL-POSED SECOND-ORDER ANISOTROPIC DIFFUSION-BASED STRUCTURAL INPAINTING SCHEME

Tudor Barbu[1], Ionuţ Munteanu[2]
[1] *Institute of Computer Science of the Romanian Academy, Iaşi, Romania*
[2] *Al.I. Cuza University, Iaşi, Romania*
tudor.barbu@iit.academiaromana-is.ro, ionut.munteanu@uaic.ro

Abstract A novel second-order nonlinear PDE-based image interpolation technique is provided in this article. It is based on a parabolic anisotropic diffusion model that is well-posed under some certain assumptions. A rigorous mathematical treatment is performed on this PDE model, the existence and uniqueness of its weak solution being investigated. An explicit finite-difference based numerical approximation scheme that is consistent to the diffusion-based model and converges to that solution is then constructed. The proposed reconstruction approach provides optimal structure-based inpainting results and works well in noisy conditions also, as resulting from our successful experiments, but is is not well-suited for textural interpolation.

Keywords: structural inpainting, well-posed PDE model, diffusivity function, finite difference method, numerical approximation scheme.
2010 MSC: 35Q68, 68U10, 94A08.

1. INTRODUCTION

Image reconstruction, known also as inpainting, completion or interpolation, represents an image analysis domain that has been widely investigated in the last decades and originates from the art restoration. It consists in the reconstruction of the missing or highly damaged regions by employing the information around them [14]. We distinguish two main categories of inpainting techniques. The texture-based interpolation methods are highly related to texture synthesis and influenced by the well-known textural inpainting aproach introduced by Efros and Leung in 1999 [2]. The structure-based interpolation algorithms use energy-based (variational) or partial differential equation (PDE) models to fulfill the inpainting task.

We could mention here some influential variational interpolation schemes, such as Mumford-Shah Inpainting model [3] and Total Variation (TV) Inpainting elaborated by Chan and Shen [14]. Some improved versions of TV Inpainting include TV Inpainting with Split Bregman [15], Blind Inpainting using l_0 and TV Regularization [16], and TV Inpainting with PDAS [7].

The second-order PDE-based inpainting schemes follow the variational principle [18], [19], while the high-order PDE inpainting algorithms do not derive from variational models, being directly given as evolutionary partial differential equations. They include third-order diffusion-based models, like CDD Inpainting [18], and fourth-order PDE-based approaches, such as Cahn-Hillard Inpainting or LCIS Inpainting [19].

The PDE-based reconstruction area is also closely related to the diffusion-based image restoration domain, numerous PDE-based interpolation approaches being derived from partial differential equation-based denoising algorithms. We have developed many such PDE-based restoration and inpainting techniques [10]–[13].

The structural inpainting scheme proposed here is based on a nonlinear second-order PDE model that can be easily derived from a variational problem. It could also be obtained from a PDE-based restoration model, by inserting an image mask corresponding to all the missing regions.

The considered parabolic anisotropic diffusion model is detailed in the next section. Then, a rigorous mathematical investigation, treating its well-posedness, is performed in the third section. Its unique and weak solution, representing the inpainting result, is computed by applying the explicit finite difference method based numerical approximation scheme described in the fourth section. The paper ends with a section of conclusions and a list of references.

2. NONLINEAR ANISOTROPIC DIFFUSION-BASED COMPLETION TECHNIQUE

If the image domain $\Omega \subseteq R^2$, let the missing zone (containing all the missing pixels of the image) be $\Gamma \subset \Omega$. The initial image that is affected by this missing region represents a partial 2D function $u_0 : \Omega \setminus \Gamma \to R$, while the evolving image is given as $u : \Omega \to R$, $u|_{\Omega\setminus\Gamma} = u_0$. One constructs an image mask for this missing region, by using the coordinates of the missing pixels and the characteristic function of that inpainting zone, Γ, which is computed as:

$$1_\Gamma(x,y) = \begin{cases} 1, & \text{for } (x,y) \in \Gamma \\ 0, & \text{for } (x,y) \notin \Gamma \end{cases} \tag{1}$$

Then, we introduce a nonlinear anisotropic diffusion-based interpolation model that successfully inpaints this region. It consists of the following second-order parabolic PDE with boundary conditions:

$$\begin{cases} \dfrac{\partial u}{\partial t} = \nabla \cdot (\varphi^u(|\nabla u|)\nabla u) + \xi(1 - 1_\Gamma)(u - u_0) \\ U(0,x,y) = u_0 \\ U(t,x,y) = 0, \text{ on } \partial\Omega \setminus \Gamma \end{cases} \tag{2}$$

where $\xi \in (0,1]$ and the diffusivity function of this PDE-based model is constructed as following:

$$\varphi^u : (0,\infty) \to (0,\infty), \quad \varphi^u(s) = \alpha \sqrt[3]{\frac{\delta_u}{\beta(s+\gamma)^k + \lambda}} \tag{3}$$

where $\alpha, \beta \in (0,1)$, $\lambda, \gamma \in [1,3]$ and $k \geq 2$.

The conductance parameter is chosen by using some statistics of the evolving image, as follows:

$$\delta_u = |\nu \cdot median(\|\nabla u\|) + \zeta \cdot \mu(\|\nabla u\|)| \tag{4}$$

where $\nu, \zeta \in (0,1)$, *median* returns the median of the argument and $\mu(\cdot)$ its average value.

This nonlinear PDE model can be derived also from a variational scheme, by solving a energy functional minimization problem. It completes the missing areas by minimizing the total variation, while keeping close to the original observation in the known regions [14]. Thus, it reconstructs the deteriorated image by directing the diffusion process mainly to its unknown zones.

The diffusivity, or edge-stopping, function is properly constructed for this diffusion. It could be easily demonstrated that it satisfies the main conditions required by a proper diffusion [14]. It is positive, since $\varphi^u(s) > 0$, $\forall s > 0$, monotonically decreasing and convergent to zero $\left(\lim_{s\to\infty} \varphi^u(s) = 0\right)$.

The inpainted image should represent the solution obtained by solving this differential model. Therefore, the existence and uniqueness of a weak solution for (2) has to be investigated. So, a rigorous mathematical treatment is performed on this second-order nonlinear anisotropic diffusion model in the following section, to analyze its well-posedness.

3. ROBUST MATHEMATICAL INVESTIGATION OF THE PDE-BASED INPAINTING MODEL

The second-order parabolic inpainting model given by (2) is now mathematically treated to determine its well-posedness. We work on the assumption that $0 < \varphi_* \leq \varphi(s) \leq \varphi^* < \infty$, $\forall s \in (0,\infty)$.

Definition 3.1. *We say that u is a weak solution to* (2) *if* $u \in C([0,T]; H_0^1(\Omega)) \cap L^2([0,T]; L^2(\Omega))$ *and*

1. $\forall \psi_1 \in H_0^1(\Omega \setminus \Gamma)$ *we have*

$$\int_{\Omega\setminus\omega} (u(T) - u_0)\psi_1 \, dx\, dy = -\int_0^T \int_{\Omega\setminus\omega} \varphi(\|\nabla u\|)\nabla u \nabla \psi_1 \, dx\, dy\, ds + \rho \int_0^T \int_{\Omega\setminus\omega} (u - u_0)\psi_1 \, dx\, dy\, ds = 0$$

2. $\forall \psi_2 \in H_0^1(\Gamma)$ *we have*

$$\int_\Gamma (u(T) - u_0)\psi_2 \, dx \, dy = -\int_0^T \int_\Gamma \varphi(\|\nabla u\|)\nabla u \nabla \psi_2 \, dx \, dy \, ds.$$

Let us consider two additional problems

$$\begin{cases} \dfrac{\partial v}{\partial t} = \nabla \cdot (\varphi(\|\nabla v\|)\nabla v) + \rho(v - u_0), \ [0,T] \times (\Omega \setminus \Gamma) \\ v = 0 \text{ on } \partial(\Omega \setminus \Gamma) \\ v(0) = u_0 \end{cases} \tag{5}$$

$$\begin{cases} \dfrac{\partial w}{\partial t} = \nabla \cdot (\varphi\|\nabla w\|\nabla w), \ [0,T] \times \Gamma \\ w = 0 \text{ on } \partial\Gamma \\ w(0) = u_0 \end{cases} \tag{6}$$

Let us firstly show that (5) has a weak solution in the sense of Definition 3.1. To this end, let any function $a = a(t,x,y)$ such that $0 < a_* \leq a(t,x,y) \leq a^* < \infty$, $\forall t, x, y$. Thus, consider the equation

$$\begin{cases} \dfrac{\partial \bar{v}}{\partial t} = \nabla \cdot (a\nabla \bar{v}) + \rho(\bar{v} - u_0), \ [0,T] \times (\Omega \setminus \Gamma) \\ \bar{v} = 0 \text{ on } \partial(\Omega \setminus \Gamma) \\ \bar{v}(0) = u_0 \end{cases} \tag{7}$$

By classical results, namely the semi-monotone argument (see [15]), equation (7) has a unique solution $\bar{v} \in ([0,T]; H_0^1(\Omega \setminus \Gamma)) \cap L^2([0,T], L^2(\Omega \setminus \Gamma)))$.

Now, let us consider the sequence (v_n) defined as $v_0 = u_0$ (the initial data)

$$\begin{cases} \dfrac{\partial v_n}{\partial t} = \nabla \cdot (\varphi\|\nabla v_{n-1}\|\nabla v_n) + \rho(v_n - u_0), \ [0,T] \times (\Omega \setminus \Gamma) \\ v_n = 0 \text{ on } \partial(\Omega \setminus \Gamma) \\ v_n(0) = u_0 \end{cases} \tag{8}$$

Since equation (8) is of the same type as (4), with $a = \varphi(\|\nabla v_{n-1}\|)$, we may conclude that, for each $n \in \mathbb{N}$, (8) has a unique solution $v_n \in C([0,T]; H_0^1(\Omega \setminus \Gamma)) \cap L^2([0,T], L^2(\Omega \setminus \Gamma))$. Scalarly multiplying (8) by v_n, we may deduce that there exists a constant $M > 0$ such that

$$|v_n|_{L^2(0,T;H_0^1(\Omega\setminus\Gamma))} \leq M, \ \left|\frac{\partial}{\partial t} v_n\right|_{L^2(0,T;H^{-1}(\Omega\setminus\Gamma))} \leq M.$$

It then follows by the Aubin Compactness Theorem for the Gelfand triple $H_0^1 \subset L^2 \subset H^{-1}$ [16], that v_n converges to some v in $L^2([0,T]; L^2(\Omega \setminus \Gamma))$, proving so that there exists a weak solution v for (2).

In the same manner as above, one may show that there exists a weak solution w for (3) also.

To conclude, since $v = w = 0$ on the common boundary, $\partial\Gamma$, we may glue them, i.e., by defining

$$u = \begin{cases} v, & \text{on } \Omega \setminus \Gamma \\ w, & \text{on } \Gamma \end{cases} \tag{9}$$

that will be a weak solution for (2).

4. NUMERICAL APPROXIMATION SCHEME

The solution of the proposed PDE model, which has been investigated in the previous section is computed by using the numerical approximation. Thus, we construct a robust numerical approximation scheme that is based on the well-known finite-difference method [17], in this section.

So, we consider a space grid size of h and the time step Δt. The space and time coordinates are quantized as:

$$x = ih,\ y = jh,\ t = n\Delta t,\ i \in \{1, ..., I\},\ j \in \{1, ..., J\},\ n \in \{0, ..., N\}. \tag{10}$$

The partial differential equation in (2) is re-written as following:

$$\frac{\partial}{\partial t} = \varphi^u(|\nabla u|)\Delta u + \nabla(\varphi^u(|\nabla u|)) \cdot \nabla u + \xi(1 - 1_\Gamma)(u - u_0). \tag{11}$$

It is then discretized by components, using the finite differences [17]. The discretization of the first component of (11) is expressed as:

$$D_1^n(i, j) = \varphi^u(|\nabla u_{i,j}^n|)\Delta u_{i,j}^n, \tag{12}$$

where the Laplacian in (12) is discretized as:

$$\Delta u_{i,j}^n = \frac{u_{i+h,j}^n + u_{i-j,h}^n + u_{i,j+h}^n + u_{i,j-h}^n - 4u_{i,j}^n}{h^2}\,. \tag{13}$$

After performing some computations, the second component can be re-written as follows:

$$\nabla(\varphi^u(|\nabla u|)) \cdot \nabla u = \varphi^{u\prime}\left(\sqrt{u_x^2 + u_y^2}\right)\ \frac{u_x^2 u_{xx} + 2u_x u_y u_{xy} + u_y^2 u_{yy}}{\sqrt{u_x^2 + u_y^2}}\,. \tag{14}$$

Then, (14) leads to the next approximation:

$$\nabla(\varphi^u(|\nabla u|)) \cdot \nabla u \approx \varphi^{u\prime}\left(\sqrt{u_x^2 + u_y^2}\right) u_{xy}(u_x + u_y), \tag{15}$$

which is then discretized as:

$$D_2^n(i, j) = \varphi^{u\prime}(|\nabla u_{i,j}^n|)\ \frac{u_{i+h,j+h}^n - u_{i+h,j-h}^n - u_{i-h,j+h}^n + u_{i-h,j-h}^n}{4h^2} \\ \frac{u_{i+h,j}^n - u_{i-h,j}^n + u_{i,j+h}^n - u_{i,j-h}^n}{2h}\,. \tag{16}$$

Therefore, the analyzed partial differential equation gets the next finite-difference based implicit numerical approximation:

$$u_{i,j}^{n+\Delta t} - u_{i,j}^{n} = D_1^n(i,j) + D_2^n(i,j) + \xi(1-1_\Gamma)(u_{i,j}^n - u_{i,j}^0) \tag{17}$$

If we consider the values $h = \Delta t = 1$, then (17) leads to the following explicit numerical approximation scheme:

$$\begin{aligned} u_{i,j}^{n+1} = \; & u_{i,j}^n(1+\xi(1-1_\Gamma)) \\ & + \varphi^u(|\nabla u_{i,j}^n|)(u_{i+1,j}^n + u_{i-1,j}^n + u_{i,j+1}^n + u_{i,j-1}^n - 4u_{i,j}^n) \\ & + \varphi^{u\prime}(|\nabla u_{i,j}^n|)\,\frac{(u_{i+1,j+1}^n - u_{i+1,j-1}^n - u_{i-1,j+1}^n + u_{i-1,j-1}^n)}{8} \\ & \cdot(u_{i+1,j}^n - u_{i-1,j}^n + u_{i,j+1}^n - u_{i,j-1}^n) - \xi(1-1_\Gamma)u_{i,j}^0 \end{aligned} \tag{18}$$

The iterative numerical approximation algorithm given by (18) is consistent to the anisotropic diffusion-based model (2) and converges quite fast to the weak solution of that PDE scheme, which represents the inpainting result. It has been successfully used in our numerical experiments that are described in the following section.

5. INPAINTING EXPERIMENTS AND METHOD COMPARISON

The developed parabolic PDE-based interpolation technique has been applied to hundreds of digital images affected by missing or highly damaged regions, very good reconstruction results being achieved. Important image collections, such as the three volumes of the USC–SIPI database, have been used in our experiments. These inpainting tests have been performed on an Intel (R) Core (TM) i7-6700HQ CPU 2.60 GHz processor on 64 bits, running Windows 10.

The interpolation results depend also on the selection of the PDE-based model's parameters. Thus, optimal completion results are achieved by using the following sequence of coefficients that are identified by the trial and error method:

$$\begin{gathered} \xi = 0.5,\ \alpha = 0.6,\ \beta = 0.4,\ \nu = 3,\ k = 2, \\ \zeta = 1.3,\ \gamma = 1.4,\ \Delta t = 1,\ h = 1,\ N = 25 \end{gathered} \tag{19}$$

Given the fast converging numerical approximation scheme described here (low number of iterations, N), the running time is usually low, however depending on the total size of the missing region and the amount of noise. The proposed inpainting algorithm provides a proper structural completion of the deteriorated image, working successfully in noisy conditions, also. Thus, it reduces the amount of the additive (Gaussian) noise, preserves the details quite well and overcomes unintended effects like blurring or staircasing [18].

The performance of our PDE-based technique has been assessed by similarity measures like Peak Signal-to-Noise Ratio (PSNR) or SSIM [19]. We have also performed inpainting method comparison. The proposed technique provides better structural interpolation results than many existing PDE-based methods, as proved by the average PSNR values registered in the next table. Unfortunately, it performs considerably weaker for texture-based image inpainting.

Table 1. Average PSNR values

Inpainting techniques	Average PSNR
This technique	32.05 (dB)
Bertalmio Inpainting	31.94 (dB)
TV Inpainting	31.35 (dB)
Perona-Malik Inpainting	29.86 (dB)
Harmonic Inpainting	27.52 (dB)

An image inpainting method comparison example is described in the following figure. The original $[512 \times 512]$ *Baboon* image is displayed in Figure 1 (a). The image affected by a missing zone and an amount of Gausian noise is depicted in (b). The image reconstructed by our diffusion-based approach is displayed in (c), the Bertalmio inpainting result in (d), the TV Inpainting output in (e), Perona-Malik inpainting result in (f) and the result provided by the linear PDE-based Harmonic Inpainting is displayed in (g).

6. CONCLUSIONS

A nonlinear anisotropic diffusion-based structural inpainting approach has been described in this work. The second-order parabolic PDE model proposed here is based on a novel diffusivity function and an inpainting mask corresponding to the missing pixels, and performs successfully the image filling process by directing the diffusion process to the missing regions, only.

The robust mathematical treatment provided here represents another original contribution of this paper. We demonstrate that the proposed differential model is well posed, admitting a unique and weak solution under some certain assumptions. We have also developed a finite difference method-based

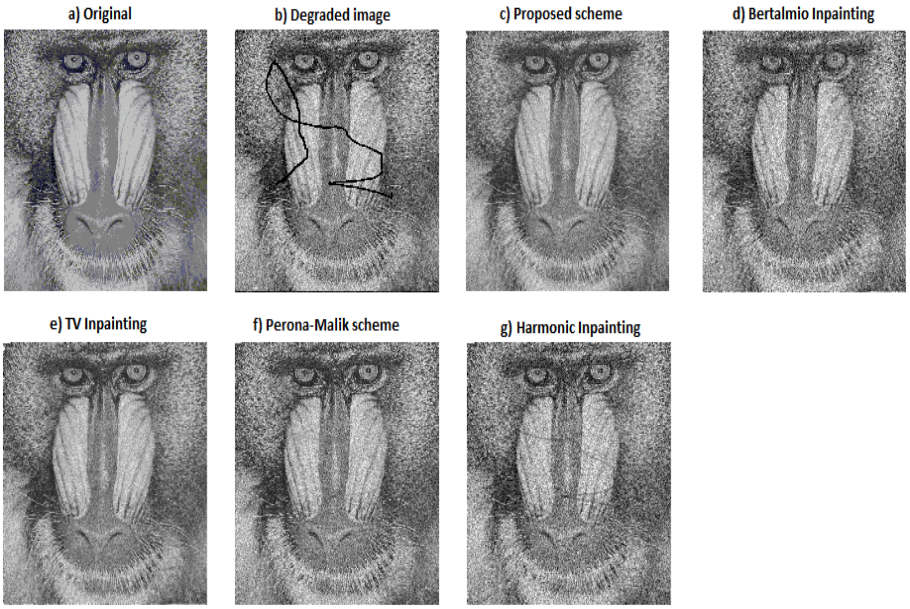

Fig. 1. Image interpolation results obtained by several methods

numerical approximation scheme to compute that PDE solution. The proposed iterative explicit numerical approximation algorithm is consistent to the anisotropic diffusion model and converges fast to its solution.

The interpolation technique introduced here outperforms many existing methods in the structural inpainting case, as resulting from the described experiments and method comparison. Unfortunately, it cannot perform properly the texture-based interpolation tasks. So, as part of our future research we intend to consider some improvements of this nonlinear diffusion-based framework, so that it becomes capable to perform both structure- and texture-based image completion. Also, new diffusivity functions and conductance parameters will be investigated for this model.

Acknowledgment. The research described in this work has been supported from the project PN-II-RU-TE-2014-4-0083/01.10.2015, which is financed by UEFSCDI Romania.

References

[1] M. Bertalmo, V. Caselles, S. Masnou, G. Sapiro, *Inpainting*, Encyclopedia of Computer Vision, Springer, 2011.

[2] A. A. Efros, T. K. Leung, *Texture synthesis by non-parametric sampling*, Proceedings of the International Conference on Computer Vision, **2**, 1999, p. 1033.

[3] M. Nitzberg, D. Mumford, *The* 2.1-*d sketch*, Proceedings of the third International Conference on Computer Vision, Osaka, Japan, 1990.

[4] T. F. Chan, J. Shen, *Morphologically invariant PDE inpaintings*, UCLA CAM Report, 2001, 1-15.

[5] P. Getreuer, *Total variation inpainting using Split Bregman*, Image Processing On Line, 2(2012), 147-157.

[6] M. V. Afonso, J. M. R. Sanches, *Blind inpainting using l_0 and total variation regularization*, IEEE Transactions on Image Processing, **24**, 7(2015), 2239-2253.

[7] M. Neri, E. R. Zara, *Total variation-based image inpainting and denoising using a primal-dual active set method*, Philippine Science Letters, **7**, 1(2014), 97-103.

[8] B. Song, *Topics in Variational PDE Image Segmentation, Inpainting and Denoising*, University of California, 2003.

[9] C. B. Schönlieb, *Partial Differential Equation Methods for Image Inpainting*, **29**, Cambridge University Press, 2015.

[10] T. Barbu, C. Moroşanu, Image restoration using a nonlinear second-order parabolic PDE-based scheme, *Analele Ştiintifice ale Universităţii Ovidius Cosntanţa*, Seria Matematică, Volume **XXV**, Fasc. 1 (2017), 33-48.

[11] T. Barbu, A. Favini, *Rigorous mathematical investigation of a nonlinear anisotropic diffusion-based image restoration model*, Electronic Journal of Differential Equations, **129** (2014), 1-9.

[12] T. Barbu, Nonlinear fourth-order diffusion-based image restoration scheme, *ROMAI Journal*, ROMAI Society, No. 1 (2016), 1-8.

[13] T. Barbu, *Variational image inpainting technique based on nonlinear second-order diffusions*, Computers & Electrical Engineering, **54** (2016), 345-353.

[14] P. Perona, J. Malik, *Scale-space and edge detection using anisotropic diffusion*, Proc. of IEEE Computer Society Workshop on Computer Vision, 1987, 16-22.

[15] V. Barbu, *Nonlinear Differential Equations of Monotone Type in Banach Spaces*, Springer, 2010.

[16] J.-P. Aubin, *Un théorème de compacité*, C. R. Acad. Sci., **256**(1963), 5042-5044.

[17] P. Johnson, *Finite Difference for PDEs*, School of Mathematics, University of Manchester, Semester I, 2008.

[18] A. Buades, B. Coll, J.M. Morel, *The staircasing effect in neighborhood filters and its solution*, IEEE Transactions on Image Processing, **15**, 6(2006), 1499-1505.

[19] K. H. Thung, P. Raveendran, *A survey of image quality measures*, Proc. of the International Conference for Technical Postgraduates (TECHPOS), 2009, 1-4.